Soft Matter

PAPER

Interactions between charged surfaces mediated by stiff, multivalent zwitterionic polymers

Klemen Bohinc,*[a] Jurij Reščič[b] and Leo Lue[c]

The interaction between like-charged objects in electrolyte solutions can be heavily altered by the presence of multivalent ions which possess a spatially distributed charge. In this work, we examine the influence of stiff, multivalent zwitterionic polymers on the interaction between charged surfaces using a splitting field theory previously shown to be accurate for the weak to the intermediate to the strong electrostatic coupling regimes. The theory is compared to Monte Carlo simulations and good agreement is found between both approaches. For surface separations shorter than the polymer length, the polymers are mainly oriented parallel to the surfaces, and the surface–surface interaction is repulsive. When the surface separation is comparable to the length of polymers, the polymers have two main orientations. The first corresponds to the polymers adsorbed onto the surface with their centers located near to or in contact with the surface; the second corresponds to polymers which are perpendicular to the charged surfaces, bridging both surfaces and leading to an attractive force between them. Increasing the surface charge density leads to more pronounced attraction *via* bridging. At surface separations greater than the polymer length, the polymers in the center of the system are still mainly perpendicular to the surfaces, due to "chaining" between zwitterions that enable them to bridge the surfaces at larger separations. This leads to an attractive interaction between the surfaces with a range significantly longer than the length of the polymers.

1 Introduction

Aqueous solutions containing charged macroions and small mobile ions appear in nearly all biological systems and biotechnological applications. Typical examples of macroions include proteins, viruses, cells, micelles, DNA molecules, actin molecules, mica, colloids, lipid membranes and silica particles. Understanding the interactions between macroions in electrolyte solutions is of fundamental importance, because they play a major role in determining the properties and behaviour of these systems. These interactions can be attractive or repulsive, depending on the surface charge density of the macroions, the structure and the valence of the mobile ions in solution.

Replacing monovalent ions with multivalent ions can lead to an effective attractive force between colloidal particles.[1,2] These attractions can cause the system to undergo phase separation.[3–5] One example is the network formation in actin solutions;[6] this is

the consequence of the attractive interactions between cytoskeletal filamentous actin molecules mediated by small multivalent ions. Another example is the condensation of negatively charged DNA molecules on zwitterionic lipid layers,[7,8] which requires the presence of divalent calcium ions. This effect has been exploited in practical applications. Divalent calcium ions are used to coagulate cement paste. Divalent diamine ions induce the aggregation of rod-like M13 viruses,[9] and divalent calcium or magnesium counterions are able to induce condensation of DNA.[10–12] Multivalent ions that are spatially extended usually show a strong tendency to induce aggregation of like-charged macroions. This is observed for positively charged colloids that condense DNA[13] or for DNA that induces attraction between cationic lipid membranes.[14]

In many colloidal solutions, the macroions are significantly larger than the coions and counterions which surround them. Consequently, the interaction between a pair of macroions can be modeled as two like-charged planar surfaces with an intervening solution. DLVO theory[15,16] has been extremely successful in describing the interaction between charged surfaces in different electrolyte solutions composed of point-like ions.

Modeling the interactions between surfaces immersed in polyelectrolyte solutions is less well developed than for the case of point charges. Wiegel[17] treated the conformational properties of a polyelectrolyte chain interacting with only one surface.

[a] Faculty of Health Sciences, University of Ljubljana, SI-1000 Ljubljana, Slovenia. E-mail: klemen.bohinc@zf.uni-lj.si; Fax: +386 1 300 1170; Tel: +386 1 300 1119
[b] Faculty of Chemistry and Chemical Technology, University of Ljubljana, SI-1000 Ljubljana, Slovenia. E-mail: jurij.rescic@fkkt.uni-lj.si; Fax: +386 1 241 9144; Tel: +386 1 479 8517
[c] Department of Chemical and Process Engineering, University of Strathclyde, James Weir Building, 75 Montrose Street, Glasgow G1 1XJ, UK. E-mail: leo.lue@strath.ac.uk; Fax: +44 141 548 2837; Tel: +44 141 548 2470

He found a structural transition between surface bound and extended configurations of the polyelectrolytes as the surface charge density changes. Miklavic and Marčelja[18] proposed a self-consistent field theory for grafted polyelectrolytes immersed in an electrolyte solution and confined between two charged walls. Åkesson, Woodward, and Jönsson[19] used a combination of Monte Carlo simulations and the Poisson–Boltzmann (PB) approach to study two charged walls embedded in a solution of oppositely charged polyelectrolytes. Their results showed that the connectivity of the chains can cause additional attractive interactions between the charged surfaces, due to the bridging of the polyelectrolytes between the walls. Podgornik investigated the forces between two charged macroscopic surfaces where the intervening medium is composed of ions and infinitely long polyelectrolytes. He demonstrated that an additional attractive force appears, even in the mean-field approximation.[20] Forsman[21] introduced a simple correlation-corrected PB theory which semi-quantitatively, and in some cases quantitatively, reproduces the net attraction between like-charged surfaces and charge reversal in electrical double layers. Also, the effect of added salt on the adsorption of polyelectrolytes onto oppositely charged surfaces and their influence on the interaction between charged surfaces have been investigated.[22]

The presence of oligomeric multivalent ions additionally enhances the magnitude of the attractive interaction between like charged colloidal particles. The bridging mechanism is responsible for the aggregation of colloidal particles by oppositely charged short polyions.[23] The forces between charged spherical aggregates conferred by oppositely charged polymeric chains have also been studied.[24] Two types of polymer mediated attractions, entropic and energetic bridging, were found.

Traditional mean-field theories, such as Poisson–Boltzmann (PB) theory, are not able to describe such systems adequately.[25] Specifically, within PB theory, the force between equally charged surfaces with intervening point ions is always repulsive. However, mean-field theories are able to describe the attraction between like-charged plates mediated by extended charge distributions, such as the polyelectrolytes with large separations between monovalent charges. In this case, the attraction arises due to intra-ionic charge correlations. These mean-field theories breakdown when the charge–charge correlations between different counterions become important. This occurs as the charge densities of the plates increase or in the limiting case of very short rod-like counterions (which approach point-like multivalent ions). Mean field theories are not able to describe such situations. These interionic correlations alone can give rise to an attraction between the like-charged surfaces.[26-29]

Complex multivalent ions with spatially separated charges are common in biological systems. Rod-like polyelectrolytes are relevant in biological applications, such as gene therapy[14,30] and biotechnology.[31] Examples of rod-like polyelectrolytes include the short polyamines, spermine and spermidine, which play an important role in DNA packaging.[11] Recently, we modeled rod-like ions between like-charged walls and demonstrated that intra-ionic correlations induced by the fixed distance between charges within a particular rod-like ion can be sufficient

to change repulsive into attractive interactions between like-charged surfaces.[32,33] It was shown that a minimum interaction energy is observed when the rod-like counterions are oriented perpendicularly to the like-charged surfaces, thus connecting surfaces via bridging.[11,34,35] The theory was validated by Monte Carlo (MC) simulations.[36-38] It was also shown that the addition of monovalent point-like salt ions causes screening that can turn the attractive interaction to repulsive.[34] The theory was extended to ions with arbitrary charge distributions along rods and within spheres.[30,39,40]

Zwitterions are molecules with both cationic and anionic groups. Depending on the solution conditions, molecules can become zwitterionic. Amino acids are the best known examples of zwitterions. Usually, membrane-forming phospholipids are zwitterions, where the polar head groups consist of anionic phosphates and cationic quaternary ammonium centers. Another simple example of a zwitterionic polymer is a uranyl ion, which was described in our previous work[41] as a rod-like ion with a spatially distributed charge. The uranium in the middle of the ion has a charge of $+2.5e_0$ (where e_0 is the fundamental unit of charge), while the oxygens at both ends of the ion have a charge of $-0.25e_0$. In this work, we investigate systems composed of multivalent zwitterionic polymers confined between two like-charged surfaces. Multiple positive and negative charges are located along the length of the zwitterionic polymers.

The remainder of this paper is organized as follows. In the next section, we describe an approximate field theory for systems of stiff, zwitterionic polymers, composed of point charges distributed along an infinitely thin rod. In this theoretical approach, the correlations between different ions, as well as the correlations within a particular ion, are taken into account. We then apply this theory to analyze the behavior of zwitterionic polymers confined between two like-charged, planar surfaces. To gain insight into this system, their properties are examined, including the electro-static potential, the ion density distributions, the orientational order parameter of the stiff zwitterions, and, in particular, the pressure between the charged surfaces. The details of Monte Carlo simulations for this system are described in the following section. In the final section, the main findings of this paper are summarized, and directions for the future work are presented.

2 Theory

In this work, we examine a system composed of two plates, one located at position $z = 0$ and the other located at position $z = D$, and each with a uniform surface charge density Σ. Between the plates is an aqueous solution of stiff, multivalent, zwitterionic polymers. This is shown schematically in Fig. 1. Each zwitterionic polymer consists of c point charges of magnitude q that are evenly spaced along its total length l. The charge density $Q(\mathbf{r}, \hat{\mathbf{n}})$ due to one of these rods, with its center located at the origin and its axis parallel to the unit vector $\hat{\mathbf{n}}$, is given by

$$Q(\mathbf{r}, \hat{\mathbf{n}}) = \sum_{k=0}^{c-1} q_k \delta^d(\mathbf{r} - (kl' - l/2)\hat{\mathbf{n}}), \quad (1)$$
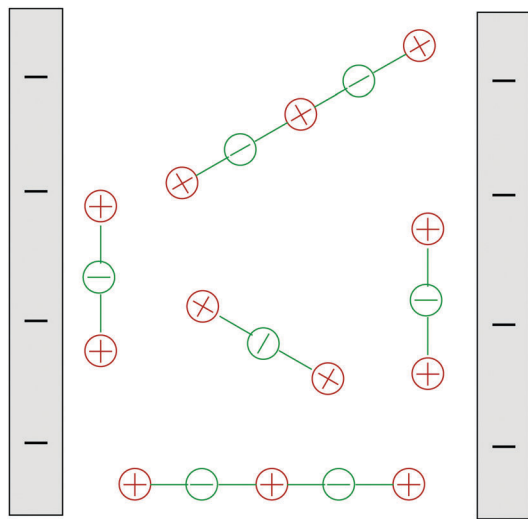
Fig. 1 Schematic illustration of the system: stiff zwitterionic polymers are embedded between two like-charged planar surfaces.

where $l' = l/(c - 1)$ is the distance between neighboring point charges, q_k is the charge of site k, and δ^d is the d-dimensional ($d = 3$) delta function.

The total charge density $\mathcal{Q}(\mathbf{r})$ in the system is

$$\mathcal{Q}(\mathbf{r}) = \Sigma \delta(z) + \Sigma \delta(z - D) + \sum_{k=1}^{N} Q(\mathbf{r} - \mathbf{R}_k, \hat{\mathbf{n}}_k),$$

where Σ is the surface charge density of each plate and D is the spacing between the plates. The second term is the charge density due to a collection of N charged polymers, where $\mathbf{R}_k$ is the position and $\hat{\mathbf{n}}_k$ is the orientation of polymer k.

The only interactions that we consider between the stiff polymers are electrostatic interactions; excluded volume and other interactions are neglected. For a system where the polymers are immersed in a solvent with a uniform dielectric constant ε, the electrostatic interaction energy E is given by

$$E = \frac{1}{2}\int d\mathbf{r} d\mathbf{r}' \mathcal{Q}(\mathbf{r}) G(\mathbf{r}, \mathbf{r}') \mathcal{Q}(\mathbf{r}) - \sum_{k=1}^{N} e^{se}(\mathbf{R}_k, \hat{\mathbf{n}}_k) \quad (2)$$

where $G(\mathbf{r},\mathbf{r}') = \varepsilon^{-1}|\mathbf{r} - \mathbf{r}'|^{-1}$ is the Green's function of the Poisson equation and $e^{se}(\mathbf{R},\hat{\mathbf{n}})$ is the self energy of a polymer:

$$e^{se}(\mathbf{R}, \hat{\mathbf{n}}) = \frac{1}{2}\int d\mathbf{r} d\mathbf{r}' Q(\mathbf{r} - \mathbf{R}, \hat{\mathbf{n}}) G(\mathbf{r}, \mathbf{r}') Q(\mathbf{r}' - \mathbf{R}, \hat{\mathbf{n}}), \quad (3)$$

which is the electrostatic interaction energy of the counterion with the electric field generated by its own charge.

In order to obtain an approximate theory for this system that is accurate in the limits when the electrostatic interactions in the system are both weak and strong, as well as for intermediate strengths, we divide the Green's function of the electrostatic interactions into short-wavelength G_s and long-wavelength G_l contributions:[29,42]

$$G(\mathbf{r},\mathbf{r}') = G_s(\mathbf{r},\mathbf{r}') + G_l(\mathbf{r},\mathbf{r}') \quad (4)$$

where $G_l = \mathcal{P}G$, and $G_s = (1 - \mathcal{P})G$, and $\mathcal{P}$ is an operator that "filters" out the short-wavelength fluctuations. The choice of this operator is fairly arbitrary, and in this work, we use $\mathcal{P} = [1 - \sigma^2\nabla^2 + \sigma^4\nabla^4]^{-1}$. The parameter σ is a length scale which distinguishes between short-wavelength and long-wavelength phenomena. Physically, this "splitting" parameter corresponds to the size of the correlation hole around each of the charges.

Using the Hubbard–Stratonovich transformation[43,44] for both the short-wavelength and long-wavelength electrostatic interactions in the system, the grand partition function of the system can be re-expressed as a functional integral over two fields, ψ_s and ψ_l, respectively. The resulting functional integration over ψ_s is evaluated by a first-order cumulant expansion, while the functional integration over ψ_l is evaluated using the mean-field approximation. Details of the derivation can be found in ref. 29 and 42 for systems of point ions and in ref. 45 and 46 for ions with extended charge distributions.

This procedure results directly in the following approximate expression for the Helmholtz free energy F of the system

$$\begin{aligned} \beta F[\rho, \Sigma] \approx &\int d\mathbf{R} d\hat{\mathbf{n}} \rho(\mathbf{R}, \hat{\mathbf{n}}) \left[\ln \rho(\mathbf{R}, \hat{\mathbf{n}}) \Lambda^3 - 1\right] \\ &- \frac{\varepsilon}{8\pi}\int d\mathbf{r} \nabla\phi(\mathbf{r}) \cdot \nabla i\bar{\psi}_l(\mathbf{r}) \\ &+ \int d\mathbf{r} \left[\Sigma(\mathbf{r}) + \int d\mathbf{R} d\hat{\mathbf{n}} \rho(\mathbf{R}, \hat{\mathbf{n}}) Q(\mathbf{r} - \mathbf{R}, \hat{\mathbf{n}})\right] i\bar{\psi}_l(\mathbf{r}) \\ &+ \int d\mathbf{R} d\hat{\mathbf{n}} \rho(\mathbf{R}, \hat{\mathbf{n}}) \beta u(\mathbf{R}, \hat{\mathbf{n}}) + \beta E_s^{se} \end{aligned} \quad (5)$$

where Λ is the de Broglie wavelength of the polymers, $\beta = 1/(k_B T)$, k_B is the Boltzmann constant, T is the absolute temperature, $\phi = k_B T \mathcal{P}^{-1}\bar{\psi}_l$ is the mean electrostatic potential of the system, and $\rho(\mathbf{R},\hat{\mathbf{n}})$ is the number density of polymers at position $\mathbf{R}$ and orientation $\hat{\mathbf{n}}$.

The first term in eqn (5) is the entropic contribution of the zwitterionic polymers to the system free energy. The second and third terms account for the (long-wavelength) energy of the electrostatic field. The fourth term is the contribution of one-body interactions $u(\mathbf{R},\hat{\mathbf{n}})$ of the polymers, which is given by

$$\begin{aligned} u(\mathbf{R}, \hat{\mathbf{n}}) = &\sum_k q_k \int d\mathbf{r}' G_s(\mathbf{R} + (kl' - l/2)\hat{\mathbf{n}}, \mathbf{r}')\Sigma(\mathbf{r}') \\ &- \frac{1}{2}\sum_{k,k'} q_k q_{k'} G_l(\mathbf{R} + (kl' - l/2)\hat{\mathbf{n}}, \mathbf{R} + (k'l' - l/2)\hat{\mathbf{n}}). \end{aligned} \quad (6)$$

The final term is the short-wavelength contribution to the electrostatic interaction energy E_s^{se}, which is given by

$$E_s^{se} = \frac{1}{2}\int d\mathbf{r} d\mathbf{r}' \Sigma(\mathbf{r}) G_s(\mathbf{r}, \mathbf{r}')\Sigma(\mathbf{r}'). \quad (7)$$

The expression for the free energy given in eqn (5) is similar to that given by Poisson–Boltzmann theory, as modified to account for rod-like counterions. The main differences are the presence of the long wavelength field $\bar{\psi}_l$, rather than the electrostatic potential ϕ, and the appearance of the two final terms,

which are not present in the Poisson–Boltzmann. As mentioned previously, the second and third terms in the free energy functional account only for the long-wavelength contributions to the energy of the electrostatic field, which is represented by $\bar{\psi}_1$. In the limit $\sigma \to 0$, $\bar{\psi}_1 \to \beta\phi$; in this case, the splitting theory reduces to the Poisson–Boltzmann equation. The short-wavelength contribution to the electrostatic energy is contained in the final two terms in the free energy; both these terms vanish when the splitting parameter approaches zero.

Given the free energy functional, all the equilibrium static properties of the system can be determined. For example, the density of the polymers is

$$
\begin{aligned}
\rho(\mathbf{R}, \boldsymbol{\Omega}) &= \frac{\delta F}{\delta\gamma(\mathbf{R}, \boldsymbol{\Omega})} \\
&= \Lambda^{-d} \exp[\gamma(\mathbf{R}, \boldsymbol{\Omega}) - \beta u(\mathbf{R}, \hat{\mathbf{n}}) \\
&\quad - \int d\mathbf{r} Q(\mathbf{r} - \mathbf{R}, \boldsymbol{\Omega}) i\bar{\psi}_1(\mathbf{r})].
\end{aligned}
\tag{8}
$$

Again, this is similar to what is found in Poisson–Boltzmann theory; however, the particle is only coupled to the slowly varying portion of the mean electrostatic potential. In addition, the short-wavelength fluctuations in the system lead to an additional one-body potential.

In order to complete the theory, we need to specify $\bar{\psi}_1$ and σ. The value of the slowly varying field $\bar{\psi}_1$ is determined by minimizing the free energy functional

$$
\frac{\delta F}{\delta\psi_1(\mathbf{r})} = 0.
\tag{9}
$$

The result is the standard Poisson–Boltzmann equation

$$
-\frac{\varepsilon}{4\pi}\nabla^2\phi(\mathbf{r}) = Q(\mathbf{r}).
\tag{10}
$$

Here Q is the total charge density of the system (due to the fixed charge and that of the mobile polymers), which is given by

$$
Q(\mathbf{r}) = \int d\mathbf{R} d\boldsymbol{\Omega} Q(\mathbf{r} - \mathbf{R}, \boldsymbol{\Omega})\rho(\mathbf{R}, \boldsymbol{\Omega})
\tag{11}
$$

While the free energy should be independent of the value of the splitting parameter, the approximate free energy (see eqn (5)) changes with σ. To minimize this artifact, the splitting parameter is chosen so that the free energy is stationary with respect to variations in σ in the first order:

$$
\frac{\partial F}{\partial\sigma} = 0.
\tag{12}
$$

Eqn (8), (10), and (12) constitute the complete description of the theory, and, in this work, they are solved numerically. The integral over the orientations of the charged polymers, which appears in the expression for the charge density, is evaluated using the trapezoid rule. The Poisson equation is solved using the finite difference method with the derivatives approximated with central differences. The long wavelength field $\bar{\psi}_1$ is computed from the mean electrostatic potential ϕ using a fast Fourier transform. In Section 4, we present the results of these calculations.

3 MC simulations

The zwitterionic polymer system was examined by NVT Monte Carlo (MC) simulations, using the integrated MC/molecular dynamics/Brownian dynamics simulation package Molsim,[47] following the standard Metropolis scheme.

The simulation box was a rectangular parallelepiped with periodic boundary conditions applied in the x- and y-directions. The dimensions of the box were $40.026 \times 40.026 \times 2.0$ nm and $40.026 \times 40.026 \times 4.0$ nm for a plate surface charge density of $\Sigma = 0.05$ C m^{-2} and $28.303 \times 28.303 \times 2.0$ nm, and $28.303 \times 28.303 \times 4.0$ nm for $\Sigma = 0.1$ C m^{-2}. The number of zwitterionic polymers was always equal to 1000, making the simulation box electrically neutral. In order to avoid the collapse of the point charges, in the MC simulations, all the point charges were surrounded by a hard sphere with a radius of 0.1 nm.

Inter-particle interactions were calculated as suggested by Jönsson et al.,[48] including the contribution to the excess internal energy caused by charges outside the simulation cell. Instead via the lattice sum technique the contribution is preferably calculated using the average charge distribution.[49]

Each trial move consists of both a random displacement and a random rotation of zwitterionic polymers. The magnitude of the displacement parameters was chosen so that the acceptance rate was approximately 50%. The simulations were started with the zwitterionic polymers randomly placed in the simulation box. 10^5 attempted moves per particle were used for equilibration runs, followed by 2×10^5 attempted moves during the production runs.

To obtain the density profiles of positive and negative charges within the zwitterionic polymers, as well as the distribution of their centers-of-mass in the direction perpendicular to the x–y plane, the z-axis was divided into 200 bins. The standard deviation of the values for each separate bin of the histograms was less than 0.5% in all cases.

4 Results and discussion

In this section, we present predictions of the field theory described previously for a system of zwitterions that are confined between two uniform negatively charged planar surfaces with the same surface charge density Σ. Two types of zwitterionic polymers are considered. The first are polymers with a total length of $l = 2$ nm that are composed of three uniformly spaced point charges: $+e_0$, $-e_0$ and $+e_0$ (where e_0 is the fundamental unit of charge). The second are polymers with a total length of $l = 2$ nm that consist of five uniformly spaced point charges: $+e_0$, $-e_0$, $+e_0$, $-e_0$, and $+e_0$.

The density profile of the polymer centers is shown in Fig. 2 for three different plate separations and three different surface charge densities. Similarly, in Fig. 3, the charge distribution is shown. The solid lines are for systems with 3-mer polymers, whereas the dashed lines are for 5-mer polymers. The distances between the charged surfaces are $D = 0.5$ nm, 2 nm and 4 nm.

For narrow plate separations (i.e. smaller than the length of the polymers), the density distribution of polymer centers
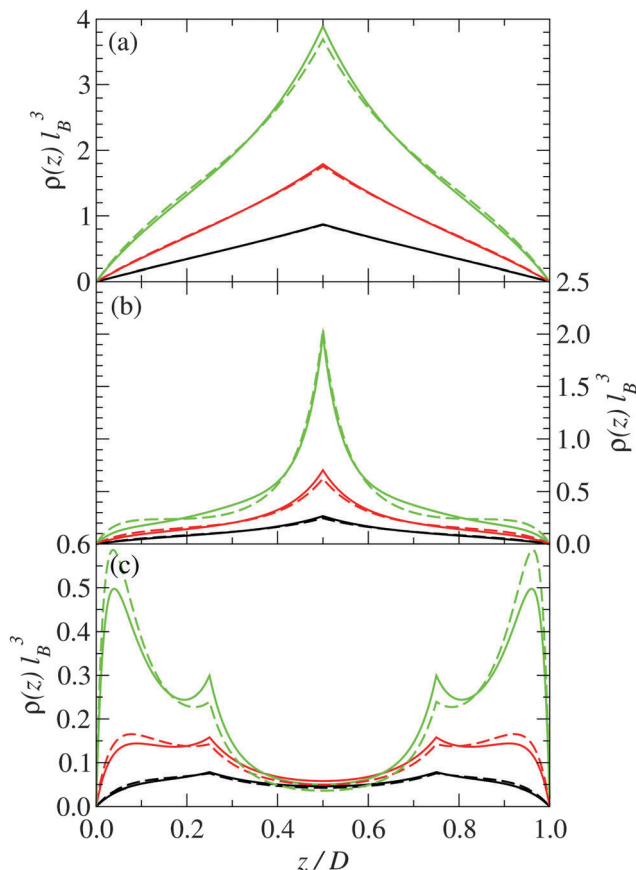
Fig. 2 Density distribution of the center of the polymers for (a) D = 0.5 nm, (b) D = 2 nm, and (c) D = 4 nm and plate surface charge densities of: (i) Σ = 0.05 C m^{-2} (black), (ii) Σ = 0.1 C m^{-2} (red), and (iii) Σ = 0.2 C m^{-2} (green). The solid lines are for stiff 3-mer polymers, and the dashed lines are for stiff 5-mer polymers.
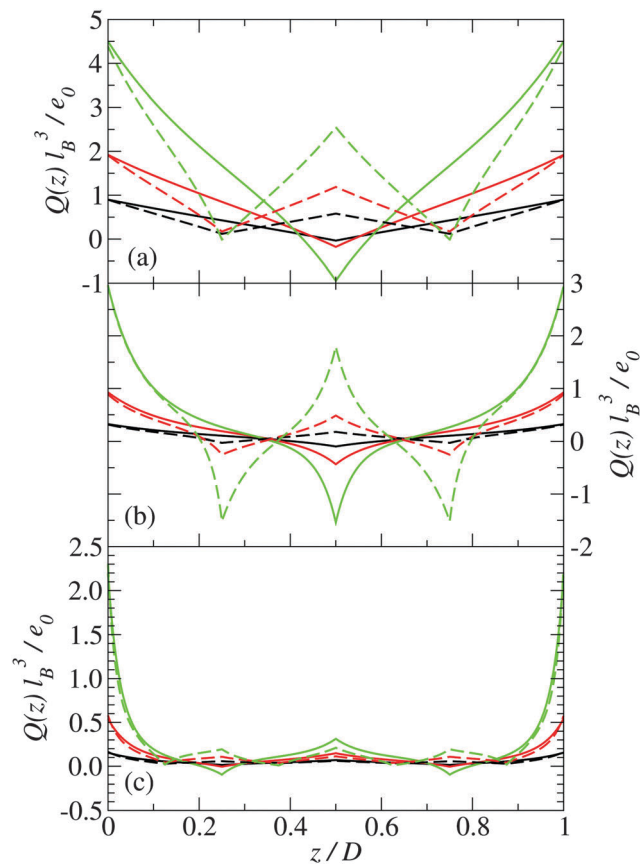

Fig. 3 Charge distribution for (a) D = 0.5 nm, (b) D = 2 nm, and (c) D = 4 nm for plate charge densities of: (i) Σ = 0.05 C m^{-2} (black), (ii) Σ = 0.1 C m^{-2} (red), and (iii) Σ = 0.2 C m^{-2} (green). The solid lines are for 3-mer stiff polymers, and the dashed lines are for 5-mer stiff polymers.

shows a pronounced peak in the middle of the system (see Fig. 2(a)). Most of the centers are located in the middle of the system. Here the orientations of the polymers are highly restricted and forced to be nearly parallel to the surface of the plates. The charge distribution in the system reflects the charge distribution on the polymers (see Fig. 3), which indicates that the polymers near the center of the system tend to be angled so that their ends are on opposite plates. This tilting is stronger at higher plate surface charge densities.

The orientation of the rod-like polymers in the system is characterized by the parameter S, which is defined as

$$S(z) = \int_{-1}^{1} d\cos\theta \left(\frac{3}{2}\cos\theta - \frac{1}{2}\right)\rho(z, \cos\theta). \quad (13)$$

where θ is the angle between a direction perpendicular to the plates and the axis of the stiff polymers. The order parameter as a function of the distance from the left plate is shown in Fig. 4. For polymers perfectly perpendicular to the plates S = 1. If the polymers are completely aligned parallel to the plates, then S = −1/2. For randomly oriented polymers the parameter S = 0.

From Fig. 4(a), we can see that at short plate separations the orientational order parameter becomes less negative as the

plate surface charge density increases, which indicates a decrease in orientational ordering. This provides further evidence that the polymers increase their tilt as Σ increases.

As the spacing between the plates increases, the density peak gradually decreases in height, however, it still remains up to the point where the separation between the plates is approximately equal to the length of the polymer. At a plate spacing equal to the length of the polymer, the polymers in the center of the system are aligned more perpendicularly to the plates, as can be deduced from Fig. 4(b). The polymer density and orientational order parameter profiles are nearly identical for both the 3-mer and 5-mer polymers. For both the 3-mer and 5-mer polymer systems, the charge distribution (see Fig. 3(b)) indicates that the positive charges are located near the surface of the plates. However, for the 3-mer polymers, the negative charges are located in the middle of the system, whereas for the 5-mer polymers, there is a positive charge at the center of the system, with negatively charged regions on either side of it. The difference in the charge density is primarily due to the difference in the charge distribution within the 3-mer and 5-mer zwitterionic polymers.

At larger separations between the plates (much larger than the length of the polymers), the distribution of the polymer
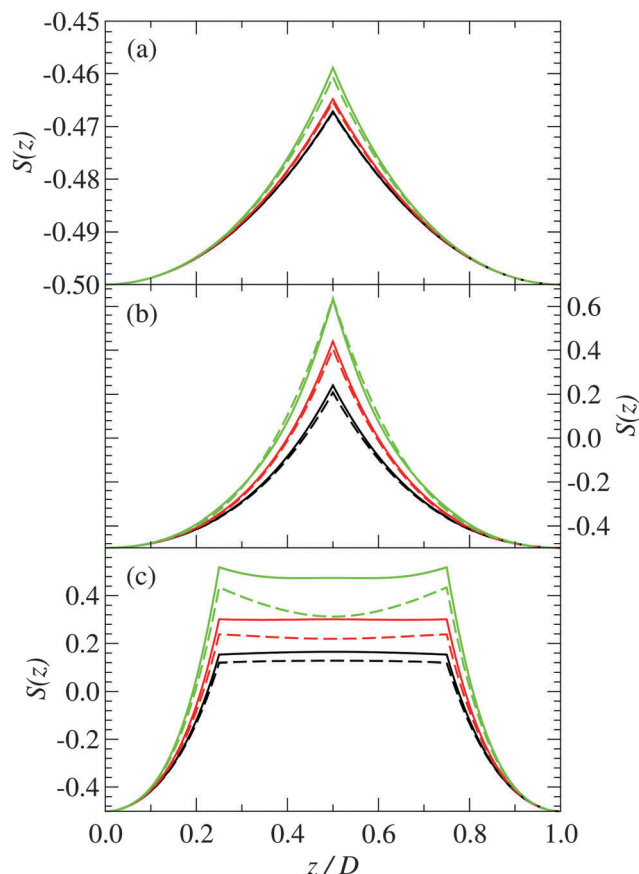
Fig. 4 Order parameter of stiff polymers confined between charged plates separated by a distance (a) D = 0.5 nm, (b) D = 2 nm, and (c) D = 4 nm for plate charge densities of: (i) Σ = 0.05 C m^{-2} (black), (ii) Σ = 0.1 C m^{-2} (red), and (iii) Σ = 0.2 C m^{-2} (green). The solid lines are for 3-mer polymers, and the dashed lines are for 5-mer polymers.

centers has pronounced peaks close to the charged surfaces. The polymers are predominately near plates and oriented parallel to the charged surfaces. The charge distribution exhibits a sharp peak of positive charge at the charged plate and a small peak in the middle of the system (Fig. 3(c)).

For both the 3-mer and 5-mer zwitterions, the charge density profiles imply that the polymers are oriented perpendicularly to the charged surfaces. This suggests a bridging mechanism of the polymers, when $D \approx l$, which holds the two planar, charged surfaces together—an effect that has been previously predicted for polyelectrolytes interacting with macroions.[50,51] This result is consistent with the often rod-like structure of common condensing agents, such as polyamines and certain linear peptides that are able to condense DNA[11,52] and other macroions.[53]

Note that this bridging mechanism appears to occur for plate separations greater than the length of the polymer. From Fig. 2(c), we can see that there are four peaks in the polymer density profile. The peaks closest to the plate surfaces correspond to polymers that are adsorbed parallel to the surfaces. The peaks farther from the surface, which occur at a distance about half of the length of the polymers, correspond to polymers that are perpendicular to the surface with one end interacting

with a surface. The polymers in the interior of the system (see Fig. 4(c)) are oriented mainly perpendicularly to the plates. This seems to be facilitated through the "chaining" of the zwitterionic polymers, with the positive charges on one polymer interacting strongly with the negative charges on another polymer. This "chaining" effect appears to be stronger in the 3-mer polymers, as they are more strongly orientated than the 5-mer polymers (see Fig. 4(c)).

Finally, we analyzed the pressure between the two charged surfaces. The pressure is calculated by taking the derivative of the free energy functional with respect to the plate separation D of the system, which leads to the expression

$$\beta p = \frac{1}{2}\sum_{k=0}^{c-1}\int_{-1}^{1} d\cos\theta\, \rho(l/2 - kl'\cos\theta, \cos\theta) - \frac{2\pi\beta}{\varepsilon}\Sigma^2 \quad (14)$$

The first term on the right is the monomer density at the surface of the left plate. The final term describes the direct electrostatic interaction energy between the plates. We plot the pressure between the charged plates as a function of their separation in Fig. 5. At separations less than the length of the zwitterionic polymers (i.e. 2 nm), the force between the plates is repulsive for all the systems examined. This is due to the entropy cost of confining the rigid zwitterions and restricting their allowed orientations.

For the lowest surface charge density, the interaction between the plates remains repulsive; however, for the higher charge densities, there is a region of attraction that extends from a separation slightly greater than the length of the polymers and to a separation roughly twice the polymer length.
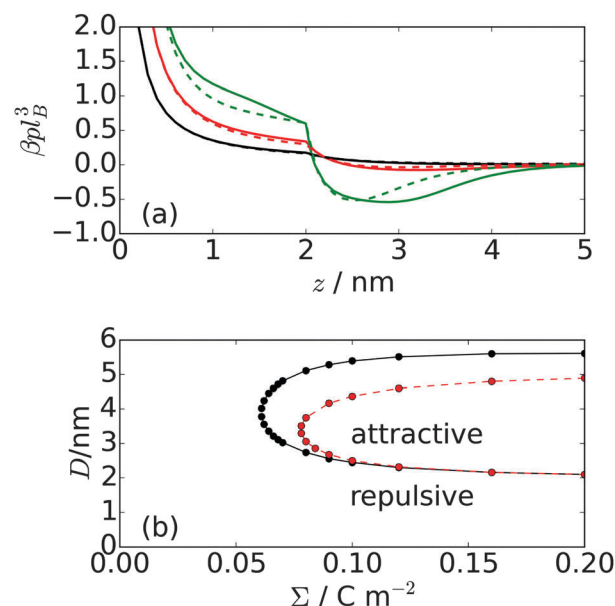

Fig. 5 (a) Pressure of a system of zwitterionic polymers confined between two similarly charged plates with surface charge densities of: (i) Σ = 0.05 C m^{-2} (black), (ii) Σ = 0.1 C m^{-2} (red), and (iii) Σ = 0.2 C m^{-2} (green). The solid curves are for 3-mer zwitterions, and the dashed curves are for 5-mer zwitterions. (b) Regions of attraction and repulsion for 3-mer (black) and 5-mer (red) zwitterionic polymers confined between two charged plates.

At larger separations, the interaction again becomes repulsive. The strength of the attraction, as well as its range, increases with increasing plate charge density. The size of the attractive region is greater for the 3-mer than for the 5-mer zwitterionic polymer. This is attributed to the stronger "chaining" effect in the 3-mer polymers, in comparison to the 5-mer polymers. The regions of attraction and repulsion for the zwitterionic polymer system are shown in Fig. 5(b). The number of polymers between the plates is fixed by the surface charge density on the plates (*i.e.* the system must be neutral overall). There are no polymers or other particles outside the plates; therefore, there are no entropic depletion forces acting on the plates. In fact, the exclusion of the polymers from the interior of the plates causes an effective repulsive force. Consequently, the regions of net attraction in the system are entirely driven by electrostatic interactions, in particular, due to correlations in the fluctuations of the charge density.

In order to assess the accuracy of the theory, we compare its predictions of the density distribution of the polymers with MC simulation results in Fig. 6 for 3-mers and those in Fig. 7 for 5-mers. The curves correspond to the theoretical predictions, and the symbols represent the MC simulation data. We find fairly good agreement between the theory and MC simulations. The deviations are due to the slight difference in the treatment of the zwitterions: the charges in the theory are point-like, while in the MC simulations, the charges are surrounded by a hard sphere of radius of 0.1 nm. Similar agreement was previously found for similar systems.[35,41,54]
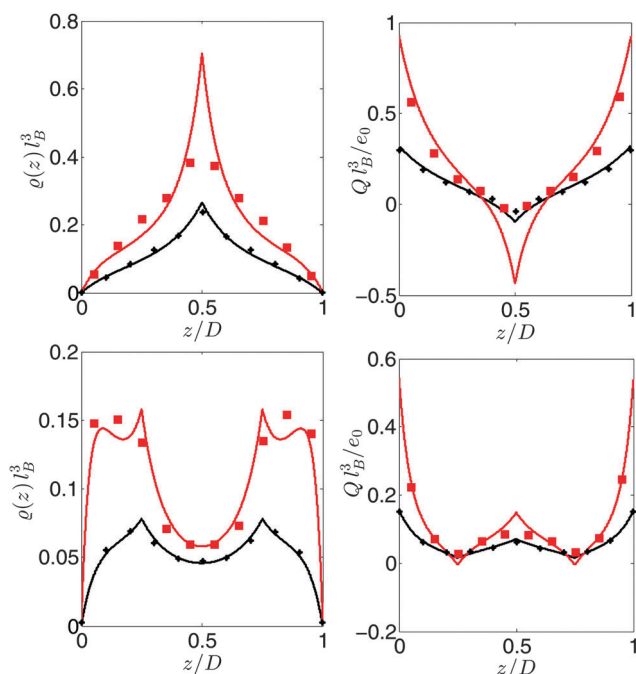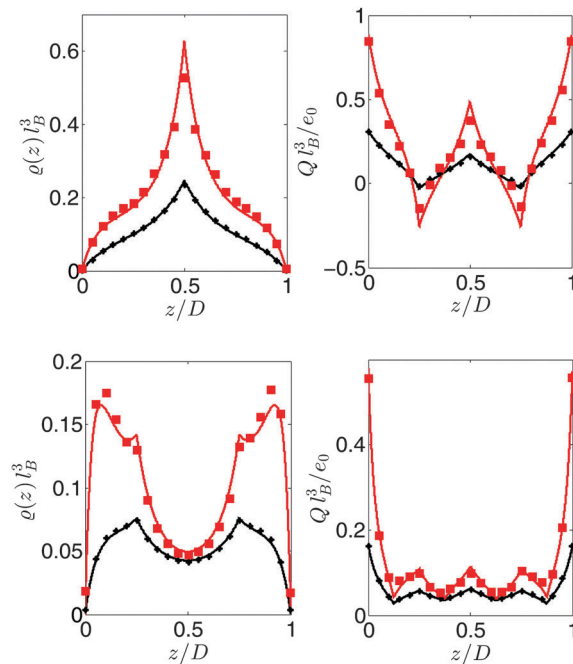

Fig. 7 Comparison between theory and MC simulations for 5-mers. The distance between the charged surfaces $D = 2$ nm (top) and $D = 4$ nm (bottom). The surface charge densities are: $\Sigma = 0.05$ C m^{-2} (black) and $\Sigma = 0.1$ C m^{-2} (red). The solid lines are the theoretical predictions, whereas the symbols correspond to MC simulation results.

5 Conclusions

In this work, we have applied an approximate field theory for zwitterionic stiff polymers confined between two parallel like-charged surfaces. The predictions of the theory were validated against MC simulations for these systems, and good agreement was found for both the polymer density and charge distributions.

When separation between the surfaces becomes comparable to the length of polymers, they are in two main orientations. The first corresponds to the polymers adsorbed onto the surface with their centers located near to or in contact with the surface. The second orientation corresponds to polymers which are oriented perpendicularly to the charged surfaces, "bridging" them. Case (b) shows a schematic illustration of the bridging mechanism, where the polymers are oriented perpendicularly to the charged surfaces.

Fig. 8 schematically summarizes the predictions of the field theory for this system. Case (a) shows a short separation between the surfaces. The polymers lie more or less parallel to the surfaces, although they are tilted such that their ends are near opposite surfaces. The entropic penalty of restricting the orientation of the polymers causes the force between the surfaces to be repulsive.

Case (c) shows a large separation between the surfaces. Polymers are adsorbed onto the left and right surfaces, and polymers in the midplane tend to be orientated perpendicularly to the surfaces. This seems to be driven by the "chaining" of zwitterionic polymers to each other, with the positive ions of one polymer interacting strongly with the negative ions of

Fig. 6 Comparison between theory and MC simulations for 3-mers. The distance between the charged surfaces $D = 2$ nm (top) and $D = 4$ nm (bottom). The surface charge densities are: $\Sigma = 0.05$ C m^{-2} (black) and $\Sigma = 0.1$ C m^{-2} (red). The solid lines are the theoretical predictions, and the symbols correspond to MC-simulation.
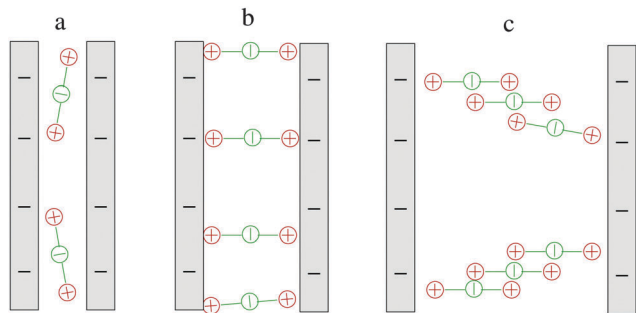
Fig. 8 Schematic illustration of three situations with different plate separations: (a) $D < l$, (b) $l = D$, and (c) $D > l$, where l is the length of rod-like zwitterionic polymers.

another. As a result, the attractive region between the plates extends to a range significantly longer than the length of the zwitterionic polymers.

This behavior differs from that observed for dimer-charges connected by infinite thin lines[46] and linear rod-like counterions composed of evenly spaced point charges.[45,55,56] For these systems, the polymers are randomly oriented in the center of the system at large plate separations, and the region of attraction does not extend too far beyond the length of the polymers.

In future, we plan to perform AFM measurements to verify these theoretical predictions with experimental systems. In real macromolecular systems, typically salt is present. Although we have not included the presence of added electrolytes in this work, the splitting theory used here is capable of accounting for this. In fact, it has already been applied to systems with multi-valent point counterions with added salts and found to yield predictions in good agreement with MC simulation results.[29] In future, we plan to investigate the influence of added mono-valent salts on the behavior of the charged rod systems. We expect that the salt will screen the charge on the macroions (charged plates), leading to a decreased interaction range and shrinking of the attractive regime.[34,57]

References

1 L. Guldbrand, B. Jönsson, H. Wennerström and P. Linse, *J. Chem. Phys.*, 1984, **80**, 2221–2228.
2 J. P. Valleau, R. Ivkov and G. M. Torrie, *J. Chem. Phys.*, 1991, **95**, 520.
3 V. Lobaskin and P. Linse, *Phys. Rev. Lett.*, 1999, **83**, 4208.
4 J. Reščič and P. Linse, *J. Chem. Phys.*, 2001, **114**, 10131.
5 L. B. Bhuiyan and C. W. Outhwaite, *J. Chem. Phys.*, 2002, **116**, 2650.
6 T. E. Angelini, H. Liang, W. Wriggers and G. C. L. Wong, *Proc. Natl. Acad. Sci. U. S. A.*, 2003, **100**, 8634–8637.
7 D. H. Mengistu, K. Bohinc and S. May, *J. Phys. Chem. B*, 2009, **113**, 12277–12282.
8 K. Bohinc, G. Brezesinski and S. May, *Phys. Chem. Chem. Phys.*, 2012, **40**, 10613–10621.
9 J. C. Butler, T. Angelini, J. X. Tang and G. C. L. Wong, *Phys. Rev. Lett.*, 2003, **91**, 028301.
10 V. A. Bloomfield, *Curr. Opin. Struct. Biol.*, 1996, **6**, 334–341.
11 V. B. Teif and K. Bohinc, *Prog. Biophys. Mol. Biol.*, 2011, **105**, 208–222.
12 K. Bohinc and L. Lue, *AIMS Biophysics*, 2016, **3**, 75–87.
13 W. M. Gelbart, R. F. Bruinsma, P. A. Pincus and V. A. Parsegian, *Phys. Today*, 2000, **53**, 38–44.
14 J. O. Radler, I. Koltover, T. Salditt and C. R. Safinya, *Science*, 1997, **275**, 810–814.
15 B. V. Derjaguin and L. D. Landau, *Acta Physicochim. URSS*, 1941, **14**, 633.
16 E. J. Vervey and J. T. G. Overbeek, *Theory of the Stability of Lyophobic Colloids*, Elsevier, Amsterdam, 1948.
17 F. Wiegel, *J. Phys. A: Math. Gen.*, 1977, **10**, 299–303.
18 S. Miklavic and S. Marčelja, *J. Phys. Chem.*, 1988, **92**, 6718–6722.
19 T. Åkesson, C. Woodward and B. Jönsson, *J. Chem. Phys.*, 1989, **91**, 2461–2469.
20 R. Podgornik, *Chem. Phys. Lett.*, 1990, **174**, 191–198.
21 J. Forsman, *J. Phys. Chem. B*, 2004, **108**, 9236–9245.
22 M. Dahlgren, A. Waltermo, E. Blomberg, P. Claesson, L. Sjostrom, T. Åkesson and B. Jönsson, *J. Phys. Chem.*, 1993, **97**, 11769–11775.
23 R. J. Hunter, *Foundations of Colloid Science*, Oxford Science Publications, Oxford, 1987, vol. 1.
24 R. Podgornik, T. Åkesson and B. Jönsson, *J. Chem. Phys.*, 1995, **102**, 9423–9434.
25 G. Cevc, *Biochim. Biophys. Acta*, 1990, **1031**, 311–382.
26 J. G. Kirkwood and J. B. Shumaker, *Proc. Natl. Acad. Sci. U. S. A.*, 1953, **38**, 863–871.
27 R. Kjellander, S. Marčelja, R. M. Pashley and J. P. Quirk, *J. Phys. Chem.*, 1988, **92**, 6489–6492.
28 Y. Levin, *Rep. Prog. Phys.*, 2002, **65**, 1577–1632.
29 M. M. Hatlo and L. Lue, *Soft Matter*, 2009, **5**, 125–133.
30 K. Bohinc, J. M. A. Grime and L. Lue, *Soft Matter*, 2012, **8**, 5679–5686.
31 S. Fodor, *Science*, 1997, **17**, 393.
32 K. Bohinc, A. Iglič and S. May, *Europhys. Lett.*, 2004, **68**, 494–500.
33 S. May, A. Iglič, J. Reščič, S. Maset and K. Bohinc, *J. Phys. Chem. B*, 2008, **112**, 1685–1692.
34 S. Maset, J. Reščič, S. May, J. I. Pavlič and K. Bohinc, *J. Phys. A: Math. Theor.*, 2009, **42**, 105401.
35 J. Reščič and K. Bohinc, *Acta Chim. Slov.*, 2015, **62**, 582–587.
36 K. B. M. A. Grime and M. O. Khan, *Langmuir*, 2010, **26**, 6343.
37 Y. W. Kim, J. Yi and P. A. Pincus, *Phys. Rev. Lett.*, 2008, **101**, 208305.
38 K. Bohinc, J. Reščič, S. Maset and S. May, *J. Chem. Phys.*, 2011, **134**, 074111.
39 S. May and K. Bohinc, *Croat. Chem. Acta*, 2011, **84**, 251–257.
40 J. G. Ibarra-Armenta, A. Martín-Molina, K. Bohinc and M. Quesada-Pérez, *J. Chem. Phys.*, 2012, **137**, 224701.
41 K. Bohinc, J. Reščič, J.-F. Dufreche and L. Lue, *J. Phys. Chem. B*, 2013, **117**(37), 10846–10851.
42 M. M. Hatlo and L. Lue, *Europhys. Lett.*, 2010, **89**, 25002.
43 R. L. Stratonovich, *Dokl. Akad. Nauk SSSR*, 1957, **115**, 1097–1100.
44 J. Hubbard, *Phys. Rev. Lett.*, 1959, **3**, 77–78.

45 M. M. Hatlo, A. Karatrantos and L. Lue, *Phys. Rev. E: Stat., Nonlinear, Soft Matter Phys.*, 2009, **80**, 061107.

46 M. M. Hatlo, K. Bohinc and L. Lue, *J. Chem. Phys.*, 2010, **132**, 114102.

47 J. Reščič and P. Linse, *J. Comput. Chem.*, 2015, **36**, 1259–1274.

48 B. Jönsson, H. Wennerström and B. Halle, *J. Phys. Chem.*, 1980, **84**, 2179–2185.

49 G. Torrie and J. Valleau, *Chem. Phys. Lett.*, 1979, **65**, 343–346.

50 H. Huang and E. Ruckenstein, *Adv. Colloid Interface Sci.*, 2004, **112**, 37–47.

51 R. Podgornik and M. Ličer, *Curr. Opin. Colloid Interface Sci.*, 2006, **11**, 273–279.

52 V. A. Bloomfield, *Biopolymers*, 1997, **44**, 269–282.

53 B. Hribar and V. Vlachy, *J. Phys. Chem. B*, 1997, **101**, 3457–3459.

54 J. Reščič and K. Bohinc, *Acta Chim. Slov.*, 2012, **59**, 601–608.

55 K. Bohinc and L. Lue, *Chin. J. Polym. Sci.*, 2011, **29**, 414–420.

56 K. Bohinc, J. M. A. Grime and L. Lue, *Soft Matter*, 2012, **8**, 5679–5686.

57 K. Bohinc and L. Lue, *Mod. Phys. Lett. B*, 2015, **29**, 1550202.